euronoise

Adaptation of the propagator for numerical acoustic holography of a wheel type object

Thibault Le Bourdon and Vincent Martin

Institut Jean Le Rond d'Alembert, UMR CNRS 7190, UPMC, 2 Place de la Gare de Ceinture, 78210 Saint-Cyr l'Ecole, France
lbourdon@ccr.jussieu.fr

The holography procedure of a vibrating object can be geometrically interpreted, resulting in a definition of the quality of the holographic process, the quality of which depends on the pressure measurement at an array of microphones and on the propagation model.
In case of a wheel with the panel body, the only possible plane array is parallel to the visible side. The velocity is then accessible on the side concerned and requires a propagation model with adequate acoustic conditions over the whole plane on that particular side (source plane).
Having in mind such a configuration, a numerical simulation in the 3D space has shown the environment influence on the reconstructed velocity on the visible side. It has appeared that vibrations, other than the ones of the front side and the rear acoustic load, can be described with admittance on the whole source plane.
We present here an exhaustive search for the adequate admittance concerned leading to the actual propagator and the actual identified velocity. The success achieved in the procedure may rely on the single model *and* single velocity liable to radiate a given pressure on a sufficiently large antenna.

1 Introduction

Among the various methods of inversion which exist in the field of the acoustic holography, experience shows that the identification of the vibratory velocity of a 3D complex object requires, in order to obtain good results, the use of a hologram not only surrounding but also taking the form of the object in the three dimensions [1, 2, 3].

When the antenna of microphones is not easy to design around the object under study (which can be the case of a car wheel surrounded with its panel body) or when we dispose only of a plane antenna of microphones, it should be noted that the object is seen by the plane antenna not as a whole but under a certain solid angle different from 4π radians. The reconstruction of the vibratory object can then only be carried out on one of its vibratory sides.

Thus, under these constraints and in order to deal with the inverse problem, the configuration in the unbounded 3D space proposed in figure 1 becomes that of figure 2 in the 3D unbounded half-space. The source plane Γ_s, limiting the domain $\Omega_{1/2\infty}$, contains on the one hand the area Γ_1 and on the other hand the complementary area Γ_s^c surrounding Γ_1. It has been demonstrated in [4] that, in these conditions, the results of the inverse problem largely depend on the boundary conditions of the entire source plane Γ_s. These conditions, revealed by the propagator which establishes a link between the vibratory velocity of the side Γ_1 and the pressure radiated on the hologram plane Γ_H, must reveal the rear acoustic load of the source plane as well as the possible vibrations on the hidden part of the vibratory source (velocity on the side Γ_2 for example). Usually idealized, Neumann or Dirichlet conditions become then insufficient [5, 6, 7].

Is it then possible to predict by holography not only the vibratory velocity of the source on its visible part from the antenna, but also the boundary conditions and thus to identify the proper propagator?

The description of the problem rests on harmonic linear acoustics and the pressure radiated can be classically obtained with the integral equation method.

An exhaustive method (taking advantage of the interpolation of the admittance in the plane of the source) will show the convergence of the optimal velocity and its associated propagator respectively towards the actual velocity and the actual propagator. This double inversion will be ensured thanks to an adapted parameter of control which represents, from a geometrical point of view, the "angle" between the vector associated with the measurement objective (the hologram) and the plane associated with the propagator. This parameter of control, making the estimation of the model possible, is not of the same type as the one which regularizes the matrices to facilitate the inherent inversion of the holography [8].

2 3D configuration and analytical resolution

The configuration (disk of radius r_1 and of thickness e which represents a wheel) given in the 3D unbounded half-space [0, +∞(, according to the axes 0y, is shown in Figure 2. The side Γ_1 of the wheel is excited by a vibratory velocity v_1 – uniform and unitary for our numerical simulations – we want to identify by using an inverse problem thanks to measurements on a hologram plane Γ_H located on $y = y_H$. These measurements are represented by the objective vector $\mathbf{p}_n$. Reminded in the introduction, and observed in [4], results of the inverse problem are dependant on the boundary conditions, revealed by the admittance β_1 on Γ_1 and β_s^c on Γ_s^c (area located in the plan Γ_s of the vibratory side and surrounding it). These conditions revealed on the one hand the "rear" acoustic load of the domain)- ∞, 0[and on the other hand the possible "hidden" sources. Thus, the side Γ_2 in y_2 is excited by uniform vibratory velocity v_2 and the "hidden" sources will be revealed, thereafter, by the ratio v_2/v_1. For the time being, the area Γ_p representing the thickness of the tyre does not have a vibratory velocity.

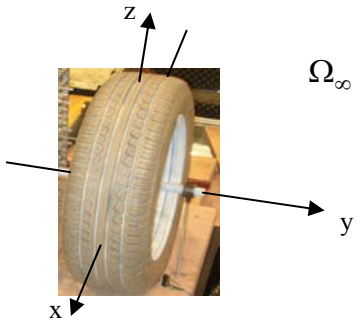

Fig.1 Representation of a car wheel in the unbounded 3D space, Ω_∞.

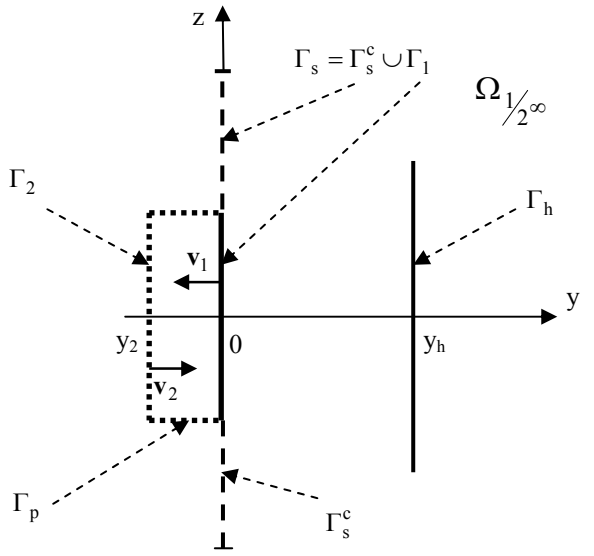

Fig.2 Configuration of the wheel of the associated problem in the unbounded half-space, $\Omega_{1/2\infty}$.

With the chosen time convention $e^{i\omega t}$ and the propagation equation $H = \Delta + k^2$, the problem in the unbounded half-space is given by the operator [4]:

$$\begin{cases} H\,p = 0 & \text{in } \Omega_{1/2\infty} \quad (1) \\ \partial_y p + i\,k\,\beta_1\,p = -i\rho\omega v_1 & \text{on } \Gamma_1 \ (\text{en } y = 0) \quad (2) \\ \partial_y p + i\,k\,\beta_s^c\,p = 0 & \text{on } \Gamma_s^c \ (\text{en } y = 0) \quad (3) \\ \partial_y p = 0 & \text{on } \Gamma_{ext} \ (\text{see hereafter}) \quad (4) \\ \text{Condition of radiation at infinity} & \end{cases}$$

The equation (4) comes from the shape of the admittance on the complementary part, Γ_s^c, of the source plane, Γ_s, where Γ_{ext} is defined by the plane (x0z) without the plane Γ_s. Indeed, it has been shown that β_s^c tends towards 0 (see Figure 4); beyond a certain limit, an homogeneous Neumann condition is reached. This condition is essential for the finite meshing of the source plane.

The objective $\mathbf{p}_n$, in the unbounded half-space, is obtained with the integral equation method. The selected elementary solution $g_{1/2\infty}(P,Q) = -e^{-ikr(P,Q)}/(2\pi r(P,Q))$ satisfies the Helmholtz equation (1) with $+\delta(P-Q)$ at the right-hand member (where P corresponds to a point source in y = 0 and Q to a receiver) and the conditions of radiation at infinity. Without any source within the domain and by including the boundary conditions, the pressure p(Q) at a point belonging to the domain $\Omega_{1/2\infty}$ can be written

$$\begin{aligned} p(Q) = {} & i\rho\omega \int_{\Gamma_1} v_n\, g_{1/2\infty}(P,Q)\, dP \\ & + ik \int_{\Gamma_1} \beta_1\, p(P)\, g_{1/2\infty}(P,Q)\, dP \\ & + ik \int_{\Gamma_s^c} \beta_s^c\, p(P)\, g_{1/2\infty}(P,Q)\, dP \end{aligned} \quad (5)$$

where v_n is given in the direct problem. The approximated numerical solution of (5) is sought with the collocation method by meshing the surface in facets. The matricial form of (5) is then

$$\mathbf{p}_n = \{p(Q)\}_{N\times 1} = \mathbf{E}(\beta_1, \beta_s^c)_{N\times M}\ \{v_n\}_{M\times 1} \quad (6)$$

where

$$\mathbf{E}(\beta_1, \beta_s^c) = i\rho\omega\left(i\,k\,\mathbf{c}^t(\beta_1, \beta_s^c)\left[\mathbf{I} - i\,k\,\mathbf{A}(\beta_1, \beta_s^c)\right]^{-1}\mathbf{B} + \mathbf{d}^t \right)$$

is the propagation model. $\mathbf{A}(\beta_1, \beta_s^c)$ is made up of the auto- and inter-influences (with principal value associated with the singularity of Green's function); $\mathbf{B}$ is the transfer of $\mathbf{v}_n$ on Γ_s; line vectors $\mathbf{c}^t(\beta_1, \beta_s^c)$ and $\mathbf{d}^t$ come respectively from the second and third terms and from the first terms of the second member of the equation (5). Finally, M is the number of points in mesh Γ_s and N is the number of points from meshing the hologram plane Γ_H.

The inverse problem is achieved with the intention of deducing the velocity v_1 on Γ_1 from measurements of the hologram points on Γ_H. Within the framework of the least square method and with appropriate hypotheses ($M \le N$ and rank($\mathbf{E}$)=M), it can be concluded that

$$\mathbf{v}_n \approx \left(\mathbf{E}^*(\beta_1, \beta_s^c)\,.\,\mathbf{E}(\beta_1, \beta_s^c)\right)^{-1}.\,\mathbf{E}^*(\beta_1, \beta_s^c)\,.\,\mathbf{p}_n \quad (7)$$

The measure gives access to the velocity of the visible source seen from the hologram. The vibratory velocity obtained is in fact the solution of the algorithms:

$$\min_{\mathbf{v}_n} \left\| \mathbf{E}(\beta_1, \beta_s^c).\mathbf{v}_n(\Gamma_s) - \mathbf{p}_n \right\|^2_{\Gamma_H}.$$

3 Interpolation of the admittance

The vibratory velocity of the source plane for specific boundary conditions is accessible with equation (7). However, for the general case, these conditions being unknown, we have on the one hand to identify the good propagation model and on the other hand to identify the vibratory velocity of the studied source.

For this purpose, it has been observed, [9], that acoustic holography is likely to be the subject of a geometrical interpretation. Indeed, results of holography are seen (see Figure 3) like resulting from the projection of the nominal objective of measurements $\mathbf{p}_n$ on the plane coming from the propagation model $\mathbf{E}(\beta_1, \beta_s^c)$; the distance $d = \left\| \mathbf{E}(\beta_1, \beta_s^c)\ \mathbf{v}_n(\Gamma_s) - \mathbf{p}_n \right\|$ is then minimal, and equal to d_{min}, and the value of $\mathbf{v}_n^{opt}$ follows. To reduce the distance d_{min} when the vector $\mathbf{p}_n$ is given, we can only act on $\mathbf{E}(\beta_1, \beta_s^c)$ (via the admittances β_1 and β_s^c) to reach the "model plane" towards the measurement objective $\mathbf{p}_n$.

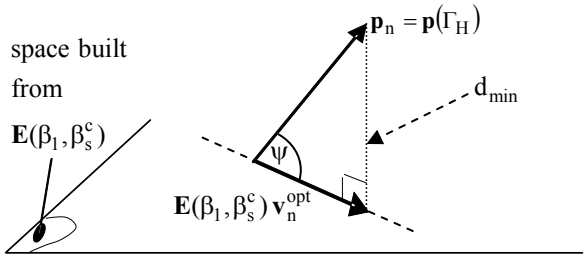

Fig.3 Geometrical representation of the acoustic holography.

Thus, it has been derived that the geometrical distance between model plane and nominal objective is revealed by:

$$\Psi = \mathrm{Arc}\sin\left(\left\|\mathbf{p}_n\right\|_{L_2} \Big/ d_{min}\right) \qquad (8)$$

Furthermore, the selected admittance is a local reaction and depends on the point. The number of unknown of the model is then directly related to the number of nodes of the plane source mesh (Γ_1 *and* Γ_s^c). It is hardly conceivable for time calculation reasons to identify each local admittance. In order to overcome this problem, let's consider that the admittance is described by a known function (by the physics of the problem *a priori*) reducing the number of the unknown to the number of coefficients of the function. The step consists then in a first stage defining a function of interpolation describing the variations of the admittance over the entire plane. The physics, revealed here by calculation in the unbounded 3D space (see figure 1), gives in figure 4 the admittance of the source plane (calculated via the finite difference method between velocities) according to radial distance r. At this point, f is equal to 250 Hz, v1 to 1, r_1 to 0.32m (wheel radius) and we consider an extreme thinness of the wheel. The studied problem is one with an axial symmetry.

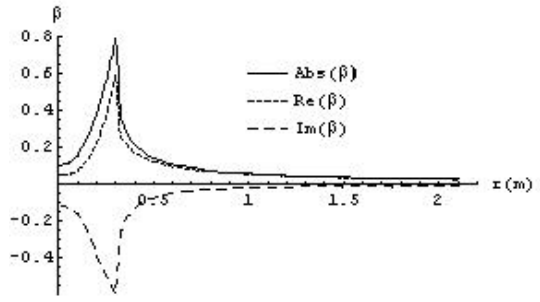

a)

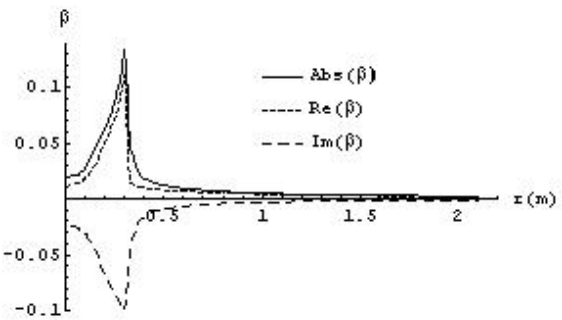

b)

Fig.4 Admittance β (absolute, real and imaginary values) calculated in the unbounded 3D space on the source plane (Γ_1 *and* Γ_s^c) - function of the radial distance r of the wheel; (a) v_2/v_1=0.2; (b) v_2/v_1=0.8.

From the shape of the admittance in Figure 4, it can be considered as a first approximation, in $\beta=\beta_R+i\beta_I$, that $\beta_R=-\beta_I$ making it possible to reduce by two the unknown of the problem. Then the interpolation function becomes $f(\beta)=(1-i)\times f(\beta_R)=(i-1)\times f(\beta_I)$.

In order to carry out a comparative study on the influence of the interpolation of the function, several interpolation functions are considered (see Table 1). For example, a first function, $f_1(\beta_R)$, describes the shape of the admittance on the vibratory part by an exponential function and on the complementary part by a $1/r$ function, thus

$$f_1(\beta_R)=\begin{cases} ae^{\alpha r} & \forall r\in[0,r_1] \\ b/r & \forall r\in[r_1,+\infty(\end{cases} \qquad (9)$$

Knowing $ae^{\alpha r_1}=b/r_1$ thus $b=r_1ae^{\alpha r_1}$ then $f_1(\beta_R)=ae^{\alpha r}$ on $[0,r_1]$ and $f_1(\beta_R)=r_1ae^{\alpha r_1}/r$ on $[r_1,+\infty($.

	$\begin{cases}\forall r\in[0,r_1]\\ \forall r\in[r_1,+\infty(\end{cases}$	Interpolation coefficients
$f_1(\beta_R)$	$\begin{cases} ae^{\alpha r} \\ \dfrac{r_1ae^{\alpha r_1}}{r}\end{cases}$	a and α
$f_2(\beta_R)$	$\begin{cases} ae^{\alpha r} \\ \dfrac{r_1^2ae^{\alpha r_1}}{r^2}\end{cases}$	a and α
$f_3(\beta_R)$	$\begin{cases} ar^2+b \\ \dfrac{r_1^2\left(ar_1^2+b\right)}{r^2}\end{cases}$	a and b
$f_4(\beta_R)$	$\begin{cases} ar^2+b \\ \dfrac{\left(ar_1^2+b-d\right)\times r_1^c}{r^c}+d\end{cases}$	a, b, c and d

Table 1 Interpolation functions of the admittance

4 Reconstruction of the velocity and the propagator by inverse problem

Having a configuration of wheel, a nominal objective issued from measurement (pressure on the hologram plane) and a model of propagation depending on the admittance, it is then possible to identify the optimal velocity on the vibratory side of the wheel from equation (7). For the following numerical simulations, the hologram plane Γ_H consists of 121 equidistant nodes (11×11), distributed symmetrically along the wheel axes (x and z), on $1m\times1m$ surface at a distance $y_H=0.12m$.

Let's consider a great number of values for each coefficient of the interpolation functions (for our simulations, the actual value is contained in the given whole). The global transfer matrix between nominal pressure and velocity of the source then becomes the hyper-matrix $\mathbf{E}(\beta_1,\beta_s^c)_{N\times M\times A\times B\times C\times D}$ where M and N have the same significance as previously and A, B, C and D are the dimensions corresponding to the selected number of values for the coefficients a, b, c and d (here, for the case of the function $f_4(\beta_R)$). Thus, for each one of the $A\times B\times C\times D$ coefficients an admittance β is calculated, defining a particular model of $\mathbf{E}(\beta_1,\beta_s^c)$. Then, for each model $\mathbf{E}(\beta_1,\beta_s^c)$, it is possible to identify the associated velocity on the vibratory area of the wheel. The figure 5 shows the identified velocity on the vibratory side Γ_1 of the wheel versus the geometrical distance, Ψ, for all the possible values of the transfer matrix $\mathbf{E}(\beta_1,\beta_s^c)$. We observe that when the model plane tends towards the nominal objective (because Ψ tends towards 0°), the identified velocity tends towards the actual one (in this case, v_1=1). Thus, the minimal angle makes it possible to deduce on the one hand the propagation model as close as possible to reality (revealed by the coefficients of the function chosen to interpolate the admittance) and on the other hand the good velocity of the source.

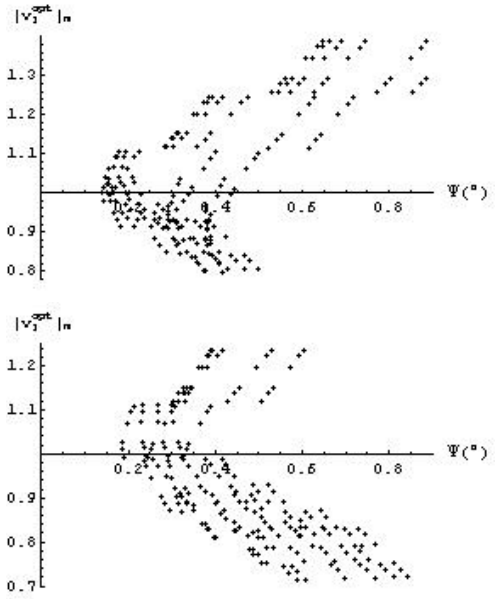

a)

b)

Fig.5 Absolute value of the average identified velocity, on the side Γ_1 of the wheel - function of the geometrical distance Ψ for each model $\mathbf{E}(\beta_1,\beta_s^c)$ built with the interpolation function $f_4(\beta_R)$;
(a) with a ratio v_2/v_1=0.6; (b) with a ratio v_2/v_1=0.4.

With the minimal value of Ψ, corresponds an interpolation function of the optimal admittance making it possible to describe as well as we can the actual value of the admittance. The figure 6 represents the optimal admittances for the different interpolation functions of table 1. The function $f_4(\beta_R)$ is the function which describes the best the actual admittance. It is noteworthy to observe that this function, needs twice more coefficients than the other interpolation functions, inevitably affecting the computing time of the hyper-matrix $\mathbf{E}(\beta_1,\beta_s^c)$. A compromise will have then to be reached between precision of the model we want to obtain (leading to the good identified velocity of the source) and the computing time.

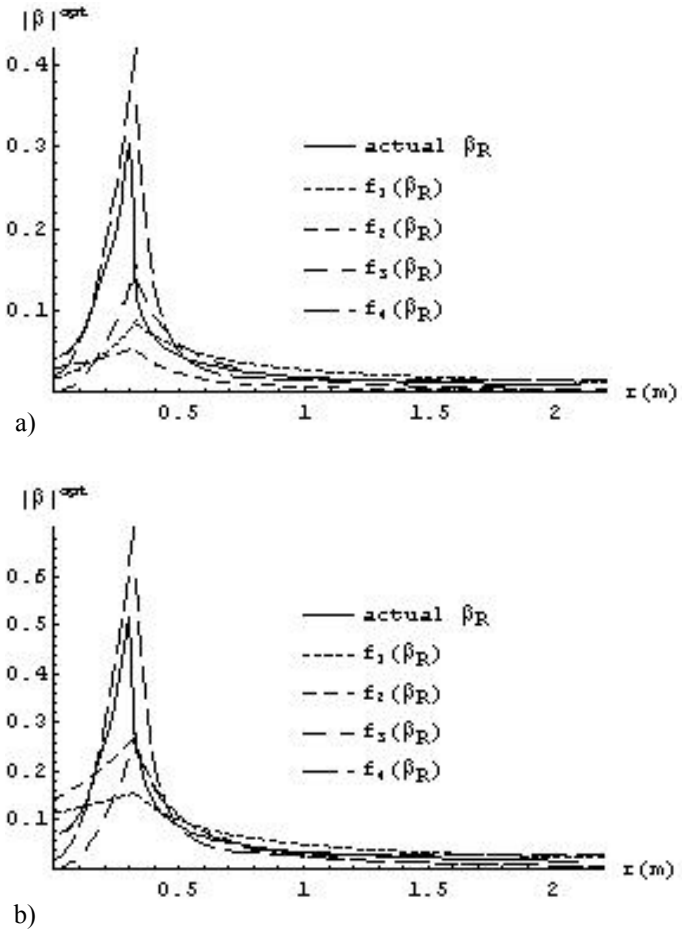

a)

b)

Fig.6 Absolute value of the optimal admittance - function of the radial distance r (in m) when the model $\mathbf{E}(\beta_1,\beta_s^c)$ corresponds to the minimal geometrical distance Ψ; comparison of the interpolation functions with the actual value calculated in the unbounded 3D space;
(a) with a ratio v_2/v_1=0.6; (b) with a ratio v_2/v_1=0.4.

Finally, the comparative study of figure 7 shows that the function $f_4(\beta_R)$ is the most adapted to identify at best the actual velocity for different rear solicitations (revealed by the ratio v_2/v_1). Intuitively, the identified velocity will have much more probabilities to reach the actual velocity with the angle Ψ decreasing. The geometrical interpretation makes sense and makes it possible, by the intermediary of a criterion (here, the geometrical distance or angle), to approach the propagation model towards the actual model and to deduce from it the vibratory velocity of the source.

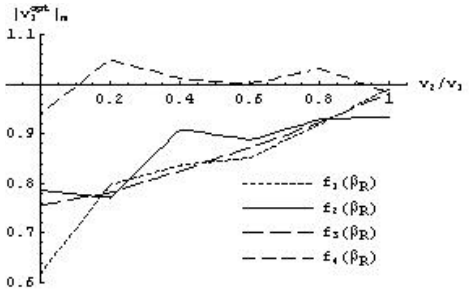

a)

b)

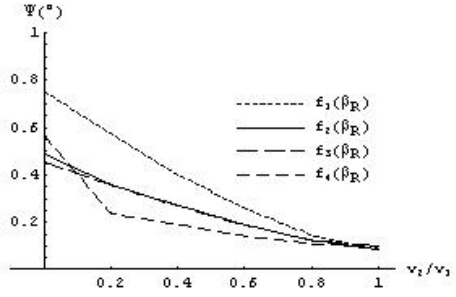

Fig.7 Results obtained with the model $\mathbf{E}(\beta_1, \beta_s^c)$ corresponding to the minimal geometrical distance - function of the ratio v_2/v_1 and for the different interpolation functions; (a) absolute value of the average of the identified velocity reconstructed on the side Γ_1 of the wheel; (b) minimal angle Ψ.

5 Conclusion

The results obtained with numerical simulations have shown at first that the identification of the vibratory velocity of a source is entirely dependant on the accuracy of the propagator.

It was then highlighted, in an exhaustive way, that it is possible to have this propagator as close as possible to the actual one, which is associated with the hologram pressure measurements. Apart from the eventual numerical problems related to the inversion of the transfer matrix, the identification of the actual propagator generates the proper reconstruction of the vibratory velocity of the source.

The convergence of the results is carried out thanks to a criterion coming from a geometrical interpretation of the acoustic holography [9]. It is then noticed that the concept of geometrical distance between the nominal vector of measurements and the plane arising from the propagation model has all its sense at the time of the identification of the velocity and the propagator.

An optimisation of the genetic algorithm type is currently set up and already shows the convergence of the system in order to identify not only the vibratory velocity but also the admittance.

This double inversion is then naturally limited by computing time. Indeed, it is not very reasonable to identify point by point the admittance on the source plane. The choice of interpolating admittance with a known function brought back the unknown of the problem to the number of coefficients of this function. This function requires knowledge of the physics of the problem prior to holographic measurements.

Simultaneously, this problem is also the object of a thorough geometrical interpretation of the acoustic holography having in view to guarantee the quality of the holographic process [10].

The authors thank the ADEME in France for funding this study within the framework of the REBECA 0566c0073 research project.

References

[1] MR. BAI, "Application of BEM (boundary element method)-based acoustic holography to radiation analysis of sound sources with arbitrarily shaped geometries ", *J. Acoust. Soc. Am.* 92,199-209 (1992)

[2] Z. Zhang, N. Vlahopoulos, S.T. Raveendra, T. Hallen, K.Y. Zhang, "A computational acoustic field reconstruction process based on an indirect boundary element formulation", *J. Acoust. Soc. Am.* 108,199-209 (2000)

[3] X. Zhao, S.F. Wu, "Reconstruction of vibro-acoustics fields using hybrid nearfield acoustic holography", *Journal of Sound and Vibration.* 282,1183-1199 (2005)

[4] V. Martin and T. Le Bourdon, "Acoustic Holography and Complementary Boundary Conditions", *Proceedings Congress ICSV14*, Cairns, Australia (2007)

[5] J.D. Maynard, E.G Williams and Y. Lee, "Nearfield Acoustic Holography; I. Theory of generalized holography and the development of NAH", *J. Acoust. Soc. Am.* 78(4),1395-1412 (1985)

[6] W.A Veronesi, J.D. Maynard, "Nearfield Acoustic Holography; II. Holographic reconstruction algorithms and computer implementation", *J. Acoust. Soc. Am.* 81(5),1307-1322 (1987)

[7] E.G. Williams and G Earl, "*Fourier Acoustics, Sound Radiation and Nearfield Acoustical Holography*", Academic Press, 183-234 (1999)

[8] Y. Kim and P.A. Nelson, "Estimation of acoustic source strength within a cylindrical duct by inverse methods", *Journal of Sound and Vibration.* 275, 391-413, (2004)

[9] V. Martin, "How accurate are results obtained by acoustic holography?", *Proceedings Congress Novem05*, Saint-Raphael, France (2005)

[10] V. Martin and C. Gronier, "Minimum attenuation guaranteed by an active noise control system in presence of errors in the spatial distribution of the primary field", *Journal of Sound and Vibration.* 217(5), 827-852, (1998)